A Boundary Conformal DG Approach for Electro-Quasistatics Problems

A. Fröhlcke, E. Gjonaj, and T. Weiland

Abstract A boundary conformal technique for solving three dimensional electro-quasistatic problems with a high order Discontinuous Galerkin method on Cartesian grids is proposed. The method is based on a cut-cell approach which is applied only on elements intersected by curved material boundaries. A particular numerical quadrature technique is applied which allows for an accurate integration of the finite element operators taking into account the exact geometry of the cut-cells. Two numerical examples are presented which demonstrate the optimal convergence rate of the method for arbitrary geometry.

1 Introduction

Staircase discretization errors for Finite Difference (FD) type discretizations on Cartesian grids represent a serious limitation on the accuracy of numerical simulations. Major efforts have been made by several authors to overcome this difficulty. Among others, the Partially Filled Cell approach for the Finite Integration Technique [1] and the Dey-Mittra conformal boundary algorithm for the Finite Difference Time Domain method [2] have been proposed. These techniques can reduce staircasing errors at curved material boundaries by incorporating explicit information on the boundary geometry into the numerical scheme. Unfortunately,

A. Fröhlcke
Graduate School of Computational Engineering, Technische Universität Darmstadt, Dolivostr. 15, 64293 Darmstadt, Germany
e-mail: froehlcke@gsc.tu-darmstadt.de

E. Gjonaj (✉) · T. Weiland
Computational Electromagnetics Laboratory, Technische Universität Darmstadt, Schloßgartenstr. 8, D-64289 Darmstadt, Germany
e-mail: gjonaj@temf.tu-darmstadt.de; thomas.weiland@temf.tu-darmstadt.de

B. Michielsen and J.-R. Poirier (eds.), *Scientific Computing in Electrical Engineering SCEE 2010*, Mathematics in Industry 16, DOI 10.1007/978-3-642-22453-9_17,

these techniques are designed specifically for low order discretizations. Indeed, high order FD methods rely on a large spatial stencil which makes the implementation of conformal boundary conditions cumbersome and numerically inefficient.

Finite Element Methods (FEM) on unstructured boundary fitted grids, on the other hand, are free of staircasing errors. These methods do provide an improved geometrical flexibility compared to FD methods. In addition, compact stencil and high order accuracy FEM can be easily formulated for a variety of electromagnetic field problems. The price due for this flexibility is a reduced numerical efficiency compared to simple FD schemes. This is directly related to the use of unstructured grids which leads to a more complicated data storage and access pattern in FEM-based computations. Furthermore, the numerical effort for generating boundary fitted unstructured grids for complex geometries can be extremely high.

In this paper, we propose a discrete formulation which combines the accuracy of high order approximations with the simple implementation and numerical efficiency of Cartesian grids. The basic idea is illustrated in Fig. 1 where a computational domain containing a single material block is discretized by a regular Cartesian grid. The material boundary subdivides several grid cells into sub-cells which are associated with (at least) two different sets of material parameters. In the following, we will refer to them as cut-cells. The challenge consists in deriving an appropriate numerical approximation within these cells. Since no general set of basis functions satisfying continuity conditions can be defined for an arbitrarily shaped cut-cell, the standard FEM formulation cannot be applied. Instead, we propose a formulation based on the high order Discontinuous Galerkin (DG) method.

As implied by the figure, the paper refers primarily to electro-quasistatics problems characterized by material parameters such as the dielectric permittivity ϵ and the electrical conductivity κ. However, the proposed discretization approach can be easily extended to other types of electromagnetic field problems. The structure of the paper is as follows. In Sect. 2, the high order DG formulation for the time-harmonic electro-quasistatics equations is introduced. In Sect. 3 the application of the boundary conformal approach with cut-cells within the framework of DG

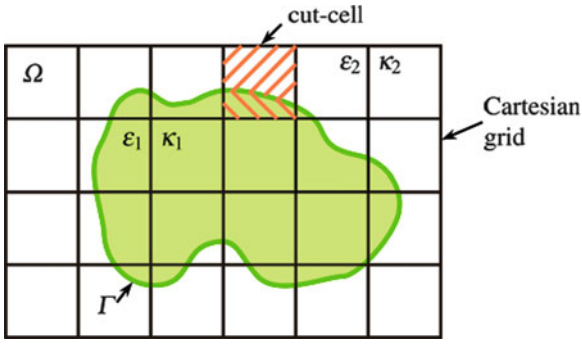

Fig. 1 Exemplary Cartesian-grid domain containing an arbitrarily shaped material block. The shaded area represents a cut-cell intersected by the material boundary

is described. The numerical accuracy and the practicability of the method are demonstrated is Sect. 4 where a simple validation example as well as the fully 3D simulation of a low frequency heating module are presented.

2 DG Formulation for Electro-Quasistatics

The time-harmonic Maxwell's equations for electro-quasistatic fields are written as:

$$\frac{1}{\epsilon}\mathbf{D}(\mathbf{x},t) = -\nabla\phi(\mathbf{x},t), \tag{1}$$

$$\mathbf{i}\omega\nabla\cdot\mathbf{D}(\mathbf{x},t) = -\nabla\cdot\left[\frac{\kappa(\mathbf{x})}{\epsilon(\mathbf{x})}\mathbf{D}(\mathbf{x},t)\right], \tag{2}$$

where ω is the angular frequency, ϕ is the electric potential, $\mathbf{D}$ is the electric flux density; ϵ and κ denote the permittivity and electric conductivity, respectively.

Given a partition of the computational domain Ω into Cartesian grid cells Ω_i, $i = 1\ldots N$ (see, e.g. Fig. 1) we introduce a discrete approximation for (1) and (2) by employing a mixed DG approach. Denoting the approximations of the electric potential and flux density by $\phi_h(\mathbf{x},t)$ and $\mathbf{D}_h(\mathbf{x},t)$, respectively, the weak problem for electro-quasistatics in the DG formulation reads: Find $\mathbf{D}_h$, ϕ_h such that

$$\int_{\Omega_i}\boldsymbol{\psi}^D_{i,q}\cdot\frac{1}{\epsilon_i}\mathbf{D}_h\,\mathrm{d}^3\mathbf{x} = -\int_{\Omega_i}\boldsymbol{\psi}^D_{i,q}\cdot\nabla\phi_h\,\mathrm{d}^3\mathbf{x}, \tag{3}$$

$$\mathbf{i}\omega\int_{\Omega_i}\psi^\phi_{i,q}\nabla\cdot\mathbf{D}_h\,\mathrm{d}^3\mathbf{x} = -\int_{\Omega_i}\psi^\phi_{i,q}\nabla\cdot\left[\frac{\kappa_i}{\epsilon_i}\mathbf{D}_h\right]\mathrm{d}^3\mathbf{x}, \tag{4}$$

$\forall i = 1\ldots N$ and $\forall q = 1\ldots P$, where P is the highest polynomial order used. In (3) and (4), $\psi^\phi_{i,q}$ and $\boldsymbol{\psi}^D_{i,q}$ represent two sets of scalar and vectorial polynomial basis functions for the electric potential and flux density, respectively. Note the index i running over all grid cells for every polynomial order q. It indicates the cell-wise definition of the DG basis functions. Thus, in contrast to the conventional FEM, the approximations obtained are, generally, discontinuous at grid cell interfaces.

Due to the discontinuous DG approximation, the evaluation of element integrals requires special attention. Considering, e.g., (3), the volume integral containing derivatives of the discontinuous electric potential is transformed as:

$$\int_{\Omega_i}\boldsymbol{\psi}^D_{i,q}\cdot\frac{1}{\epsilon_i}\mathbf{D}_h\,\mathrm{d}^3\mathbf{x} = -\int_{\Omega_i}\phi_h\nabla\cdot\boldsymbol{\psi}^D_{i,q}\,\mathrm{d}^3\mathbf{x} + \int_{\partial\Omega_i}\tilde{\boldsymbol{\phi}}_h\boldsymbol{\psi}^D_{i,q}\cdot\mathbf{n}\,\mathrm{d}^2\mathbf{x}. \tag{5}$$

In (5), $\tilde{\phi}_h$ denotes the *numerical flux* for the electric potential defined at the cell interface and $\mathbf{n}$ is the outward pointing interface normal. In order to complete the

DG formulation (3)–(5), a numerically consistent relation for these fluxes must be provided. Several possibilities exist for defining them (see, e.g., [3] for a complete review of choices). In the numerical examples presented below, the so called central flux scheme for the electric potential as well as for the flux density is applied.

Expressing the field approximations ϕ_h and $\mathbf{D}_h$ by means of the basis functions $\psi^{\phi}_{i,q}$ and $\boldsymbol{\psi}^{D}_{i,q}$, respectively, and evaluating the integrals (3) and (4) using numerical fluxes as in (5), yields the set of matrix equations:

$$\mathbf{M}\mathbf{I}_{1/\epsilon}\mathbf{d} = -\mathbf{G}\boldsymbol{\phi} + \mathbf{f}_{\phi}, \tag{6}$$

$$\mathbf{i}\omega\mathbf{G}^T\mathbf{d} = -\mathbf{G}^T\mathbf{I}_{\kappa/\epsilon}\mathbf{d} + \mathbf{f}_d, \tag{7}$$

where $\mathbf{G}$ is the discrete gradient operator, $\mathbf{M}$ is the mass matrix, $\mathbf{I}_{1/\epsilon}$ and $\mathbf{I}_{\kappa/\epsilon}$ are diagonal matrices containing the cell-wise constant material parameters and $\mathbf{f}_{\phi}$ and $\mathbf{f}_d$ are vectors of boundary conditions. Equations (6) and (7) can be further reduced by a Schur complement approach resulting in

$$-\mathbf{G}^T\left(\mathbf{i}\omega\mathbf{I}_{\epsilon} + \mathbf{I}_{\kappa}\right)\mathbf{M}^{-1}\mathbf{G}\boldsymbol{\phi} = \mathbf{f}_d - \mathbf{G}^T\left(\mathbf{i}\omega\mathbf{I}_{\epsilon} + \mathbf{I}_{\kappa}\right)\mathbf{M}^{-1}\mathbf{f}_{\phi}. \tag{8}$$

The above equation can be solved for the potential degrees of freedom $\boldsymbol{\phi}$ using an iterative or direct solver for complex symmetric systems. The Schur complement reduction in (8) can be trivially applied since the mass matrix $\mathbf{M}$ in the DG formulation is block-diagonal. The choice of the basis functions $\psi^{\phi}_{i,q}$ and $\boldsymbol{\psi}^{D}_{i,q}$ is, generally, uncritical for DG-type discretizations. In this work, the high-order hierarchical basis functions proposed in [4] is used. The definition of the electric potential basis functions in the reference element is identical with that employed in H^1-conforming FEM. Correspondingly, the flux density within each element is approximated using a set of high order basis functions which coincides with that used in $H(div)$-conforming FEM (cf. [4]). The reason for this choice is to maintain some degree of equivalence with the standard FEM for comparison and (possibly) hybridization purposes. Note, however, that DG can be neither H^1- nor $H(div)$-conforming, since the global approximation is generally discontinuous.

3 Cut-Cell Approach

The basic observation is that the above derivation does not depend on cell (element) geometry. In particular, it can be applied on the cut-cells of a Cartesian grid as shown in Fig. 1. The latter can be considered as independent grid cells characterized by a unique material. The weak DG equations for the cut-cells can be formally written as in (3) and (4) for the standard (Cartesian) cells provided that, for each cut-cell, a set of independent approximation functions, $\psi^{\phi}_{c,q}$ and $\boldsymbol{\psi}^{D}_{c,q}$, is specified. Thus, the cut-cell approach can be interpreted as a modification of the original Cartesian grid to

include additional cells of arbitrary curved geometry. This modification, however, is applied only in the vicinity of material boundaries corresponding to the splitting of the original Cartesian grid cells into several cut-cells with different material content.

In the present implementation, the approximation functions within the cut-cells are chosen to be identical with those in the parent Cartesian cell. This choice is independent from the geometry of the cut-cell, since the DG formulation does not impose conformity constrains on these functions; not even for the regular grid cells away from material boundaries. The field discontinuity at the boundary surface between two neighboring cut-cells is treated naturally within the DG framework by introducing numerical fluxes as in (5).

The numerical evaluation of the DG integrals, however, needs an appropriate description for the cut-cell geometry. For this purpose, the Open CASCADE geometry kernel [5] is used. It enables a geometrical representation of the cut-cells based on parametrized Bezier and B-Spline surfaces. Furthermore, high order Gauss quadrature rules for evaluating surface integrals are provided. Internal integral terms require a separate treatment. Referring again to the weak equation (3) for a cut-cell volume Ω_c, the following transformations are performed:

$$\begin{aligned}\int_{\Omega_c} \boldsymbol{\psi}^D_{c,q} \cdot \frac{1}{\epsilon_c}\mathbf{D}_h \, \mathrm{d}^3\mathbf{x} &= -\int_{\Omega_c} \phi_h \nabla \cdot \boldsymbol{\psi}^D_{c,q} \, \mathrm{d}^3\mathbf{x} + \int_{\partial\Omega_c} \tilde{\boldsymbol{\phi}}_h \boldsymbol{\psi}^D_{c,q} \cdot \mathbf{n} \, \mathrm{d}^2\mathbf{x} \\ &= \int_{\partial\Omega_c} \left(-\mathbf{S}^D_{c,q} + \tilde{\boldsymbol{\phi}}_h \boldsymbol{\psi}^D_{c,q}\right) \cdot \mathbf{n} \, \mathrm{d}^2\mathbf{x}, \end{aligned} \tag{9}$$

where $\mathbf{S}^D_{c,q}$ is a primitive function of the integrand in the first integral term defined by the relation, $\nabla \cdot \mathbf{S}^D_{c,q} = \phi_h \nabla \cdot \boldsymbol{\psi}^D_{c,q}$. Since a polynomial basis approximation is assumed, $\mathbf{S}^D_{c,q}$ can be determined analytically for arbitrarily high orders. Thus, the weak formulation integrals (3) and (4) can be fully reduced to surface integrals along the cut-cell faces which can be further evaluated by the numerical quadrature rules provided by the geometry kernel.

4 Numerical Examples

4.1 Validation

The simple model of a cylindrical capacitor filled with an electrically conducting material is considered (see Fig. 2). For simplicity, a time independent setup is assumed. It consists in a constant voltage excitation applied between the inner and outer electrodes of the capacitor. Thus, the problem reduces to a stationary current flow problem with exact analytical solution which can be used for investigating the accuracy of the method.

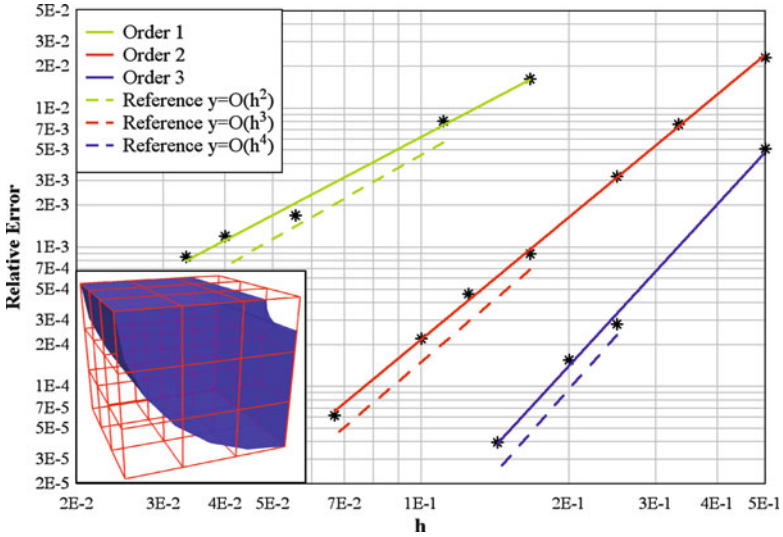

Fig. 2 Relative error measured in the L2-norm of electric potential vs. mesh parameter for different DG approximation orders

Figure 2 shows the numerical error for the electric potential vs. grid resolution for different DG approximation orders. Obviously, the numerical result converges with the optimal convergence order, $P+1$, where P is the highest degree of polynomials used in the approximation. The cut-cell approach is, thus, exact in the sense that, for arbitrarily curved geometry, it does not introduce additional numerical errors (like staircasing errors) apart for the usual approximation error of DG. In the simulations, uniform and comparatively sparse Cartesian grids with 2–30 cells along the side of the computational domain were used.

4.2 Simulation of a Heating Module

As a real world example, the simulation of a heating module is considered (see Fig. 3). The device is commonly used in the food processing industry to improve the shelf life of liquid products such as milk or juice [6]. It consists of two steel electrodes embedded in a teflon case and operated at 250 kHz. The model dimensions are $20 \times 20 \times 20$ cm with rectangular electrodes of side length 13.5 cm. The fluid flowing between the electrodes is assumed to be orange juice with an electrical conductivity of $0.5\,\mathrm{S/m}$ and a relative permittivity of 80. The conductivity and relative permittivity of teflon are assumed to $10^{-12}\,\mathrm{S/m}$ and 3, respectively.

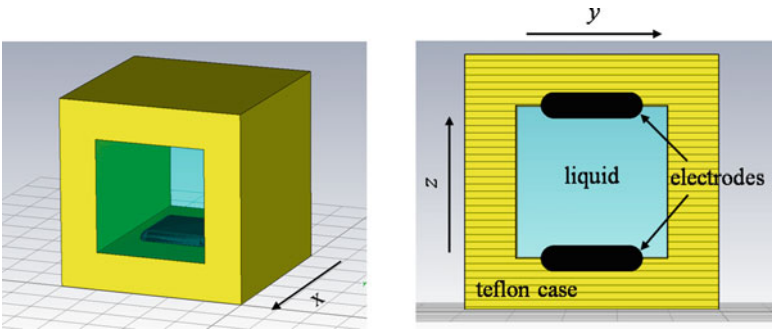

Fig. 3 *Left*: Geometry of the heating module. *Right*: Cross sectional view of the device

The rectangular problem geometry suggests the use of a Cartesian grid. Exceptions make the two electrodes having rounded edges to avoid local peaks in the electric field distribution. The situation can be well handled by the cut-cell approach, since only a small number of cut-cells along the electrode surfaces needs to be considered. In the present simulation, a uniform Cartesian grid with $10 \times 10 \times 10$ cells is used. For the numerical field solution the high order cut-cell DG approach with quadratic basis functions is applied.

Figure 4 shows some of the field distributions obtained by simulation on several cross-sections of the heating module. Note the high resolution of the electric potential and current density obtained in the vicinity of the electrodes, although, an extremely sparse regular grid is used. This accuracy is due to the high order approximation of the DG formulation combined with the cut-cell approach presented in the paper. The heating module example demonstrates the capability of the method to handle practical problems efficiently on simple Cartesian grids by completely avoiding staircasing errors which are typical for FD based methods.

5 Conclusions

A cut-cell approach for the high order DG method is proposed. The method is derived for the case of time-harmonic electro-quasistatics problems, although, it can be easily applied for the solution of other types of static or time dependent electromagnetic field problems. The strength of this approach consists in its capability to obtain high order accuracy solutions on trivial meshes. The discrete problem formulation is simple and easy to implement. This is because the cut-cell approach can be naturally embedded within the DG framework which does not impose conformity conditions on the approximation spaces. The validation example presented in the paper shows that this approach converges at optimal rate for any approximation order.

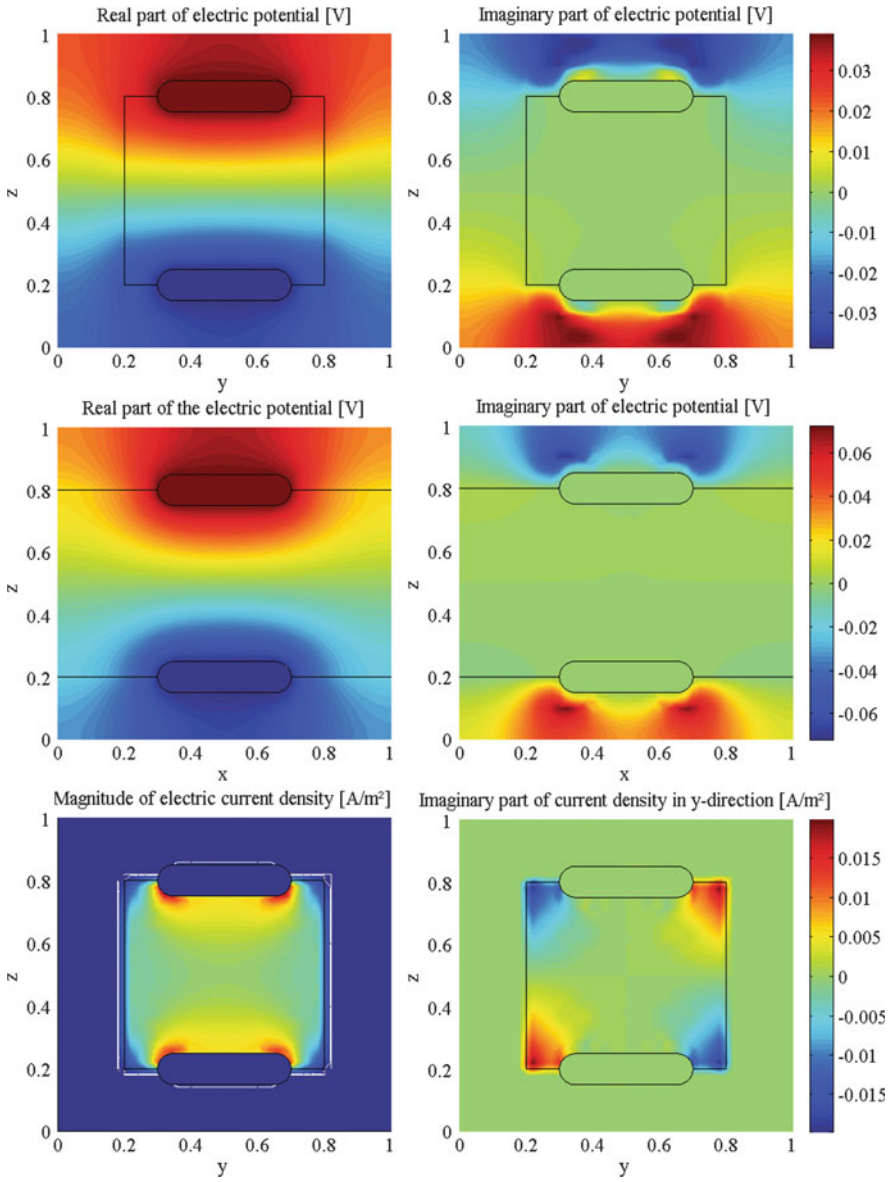

Fig. 4 *Top*: Real and imaginary part of the normalized electric potential on the yz-plane. *Middle*: Real and imaginary parts of the normalized electric potential on the xz-plane. *Bottom*: Magnitude (*left*) and imaginary part of the y-component of the current density on the yz-plane

References

1. Thoma, P.: Zur numerischen Lösung der Maxwellschen Gleichungen im Zeitbereich. PhD Dissertation, TU Darmstadt (1997)
2. Dey, S., Mittra, R.: A locally conformal finite-difference time-domain (FDTD) algorithm modeling modeling three-dimensional perfectly conducting objects IEEE Microw. Guid. Wave Lett. **7**, 273–275 (1997)
3. Arnold, D.N., Brezzi, F., Cockburn, B., Marini, D.: Unified analysis of discontinuous Galerkin methods for elliptic problems. SIAM J. Numer. Anal. **39**, 1749–1779 (2002)
4. Schöberl, J., Zaglmayr, S.: High order Nedelec elements with local complete sequence properties. COMPEL **24**, 374–384 (2005)
5. OpenCascade 4.0, Open-Source Toolkit for 3D modeling (2001). URL: http://www.opencascade.com
6. Scholler, C., et al.: Numerical simulation of thermally coupled electromagnetic fields and fluid flow. In: Proceedings of Computational Methods for Coupled Problems in Science and Engineering, Papadrakakis, M., Onate, E., Schreffler, B. (eds.) CIMNE, Barcelona (2005), Santorini, Greece, May 2005